BBA - Molecular Basis of Disease 1868 (2022) 166562

Contents lists available at ScienceDirect

BBA - Molecular Basis of Disease

journal homepage: www.elsevier.com/locate/bbadis

TLR4 activation induces inflammatory vascular permeability via Dock1 targeting and NOX4 upregulation

Jin H. Song [a], Joseph B. Mascarenhas [a], Saad Sammani [a], Carrie L. Kempf [a], Hua Cai [b], Sara M. Camp [a], Tadeo Bermudez [a], Donna D. Zhang [c], Viswanathan Natarajan [d], Joe G.N. Garcia [a,*]

[a] Department of Medicine, University of Arizona Health Sciences, Tucson, AZ, United States of America
[b] Department of Anesthesiology. University of California Los Angeles, Los Angeles, CA, United States of America
[c] Department of Pharmacology and Toxicology, University of Arizona Health Sciences, Tucson, AZ, United States of America
[d] Department of Pharmacology, University of Illinois at Chicago, Chicago, IL, United States of America

ARTICLE INFO

Keywords:
Dock1
EC barrier integrity
Elmo1
eNAMPT
Oxidative stress
Vascular permeability

ABSTRACT

The loss of vascular integrity is a cardinal feature of acute inflammatory responses evoked by activation of the TLR4 inflammatory cascade. Utilizing in vitro and in vivo models of inflammatory lung injury, we explored TLR4-mediated dysregulated signaling that results in the loss of endothelial cell (EC) barrier integrity and vascular permeability, focusing on Dock1 and Elmo1 complexes that are intimately involved in regulation of Rac1 GTPase activity, a well recognized modulator of vascular integrity. Marked reductions in Dock1 and Elmo1 expression was observed in lung tissues (porcine, rat, mouse) exposed to TLR4 ligand-mediated acute inflammatory lung injury (LPS, eNAMPT) in combination with injurious mechanical ventilation. Lung tissue levels of Dock1 and Elmo1 were preserved in animals receiving an eNAMPT-neutralizing mAb in conjunction with highly significant decreases in alveolar edema and lung injury severity, consistent with Dock1/Elmo1 as pathologic TLR4 targets directly involved in inflammation-mediated loss of vascular barrier integrity. In vitro studies determined that pharmacologic inhibition of Dock1-mediated activation of Rac1 (TBOPP) significantly exacerbated TLR4 agonist-induced EC barrier dysfunction (LPS, eNAMPT) and attenuated increases in EC barrier integrity elicited by barrier-enhancing ligands of the S1P1 receptor (sphingosine-1-phosphate, Tysiponate). The EC barrier-disrupting influence of Dock1 inhibition on S1PR1 barrier regulation occurred in concert with: 1) suppressed formation of EC barrier-enhancing lamellipodia, 2) altered nmMLCK-mediated MLC2 phosphorylation, and 3) upregulation of NOX4 expression and increased ROS. These studies indicate that Dock1 is essential for maintaining EC junctional integrity and is a critical target in TLR4-mediated inflammatory lung injury.

1. Introduction

The loss of lung vascular barrier integrity, resulting in vascular leakage, alveolar flooding, and respiratory failure, are critical pathobiological features of the acute respiratory distress syndrome (ARDS), a life-threatening inflammatory condition in the critically ill [1–3]. Lung vascular permeability in ARDS is directly related to excessive generation of reactive oxygen species (ROS) and activation of innate immunity inflammatory cascades, including Toll-like receptor 4 (TLR4) signaling cascade, triggered by ligation of the pathogen recognition receptor, TLR4, by the bacterial product, lipopolysaccharides (LPS). LPS is the endotoxin derived from the outer membrane of gram-negative bacteria that disrupts the alveolar-capillary barrier, resulting in a pulmonary vascular leak. LPS triggers TLR4 signaling to induce massive inflammation to produce acute sepsis and ARDS. Secretion of the damage-associated molecular pattern protein, eNAMPT (extracellular nicotinamide phosphoribosyltransferase), acts as a master regulator of inflammatory networks via binding to TLR4, eliciting profound NFκB-mediated inflammatory cytokine release [4–6]. Like LPS, eNAMPT ligation of TLR4 produces a significant loss of EC barrier integrity, resulting in increased vascular permeability [7,8] and tissue inflammatory injury. Our preclinical and human studies have highlighted eNAMPT/TLR4 signaling as a critical contributor to the severity of inflammatory lung injury induced by excessive mechanical ventilation and

* Corresponding author at: University of Arizona Health Sciences, United States of America.
E-mail address: skipgarcia@email.arizona.edu (J.G.N. Garcia).

https://doi.org/10.1016/j.bbadis.2022.166562
Received 1 April 2022; Received in revised form 30 August 2022; Accepted 22 September 2022
Available online 27 September 2022

bacterial and viral infections, including infection with SARSCoV2 [9–11]. We recently demonstrated that minipigs and rats exposed to septic shock and mechanical ventilation-induced lung injury (VILI) display profound lung inflammation, cytokine production, and vascular leakage into the lungs. These events depend upon eNAMPT/TLR4 signaling [7,11]. As eNAMPT-neutralizing humanized monoclonal antibody (mAb), ALT-100 significantly relieved eNAMPT- and LPS-induced declines in endothelial cell (EC) barrier integrity in vitro and dramatically attenuated LPS/VILI severity in murine, rat, and porcine models [7,11].

The exact mechanism by which the TLR4 inflammatory cascade elicits profound increases in vascular permeability is incompletely understood, and critical mechanistic gaps remain. Recent studies indicate that TLR4 activates the ion channel, Piezo1, to generate ROS and cytoskeletal alterations in a Rac GTPase-dependent manner [12]. NADPH oxidase is a primary source of ROS generation in ECs [13] and is controlled by the GTP/GDP state of the Rac GTPase [14,15]. In pulmonary ECs, VEGF-mediated activation of Rac1 caused ROS generation that was inhibited by NADPH oxidase inhibition [16]. NOX4 is a key ROS producing target implicated in the pathogenesis of both sepsis and ARDS [17,18]. In this study, Nox4 deficiency in mice, but not deficiency of either Nox1 or Nox2, significantly attenuated LPS-induced ROS production and improved survival in sepsis-induced acute lung injury. Alternatively, studies that enhance Nrf2-target antioxidants to ameliorate acute lung injury suggest that excessive ROS generation is implicated in sepsis/ARDS [19].

Previously, we have shown the extensive involvement of Rac1 GTPase in EC barrier preservation, recovery, and gap closure [20–22] elicited by a barrier–enhancing agonists (S1P/TySIPonate). In addition to the importance of S1PR1 signaling to vascular development [23], both S1P- and TySIPonate-induced S1PR1 signaling catalyzes actin cytoskeleton rearrangements, formation of a peripheral actin ring (to anchor cellular junctions), focal adhesion remodeling and increased lamellipodia formation that is designed to close paracellular gaps and enhance vascular integrity [24,25]. Rac1 is preferentially activated at the leading edge of migrating cells, where it induces the formation of actin-rich lamellipodia protrusions thought to be a key driving force for membrane extension and cell movement [6,26]. Thus, the loss of regulatory molecules involved in Rac1 activity potentially severely alters cell movement and cytoskeletal actin rearrangements. We and others have shown that Rac1 inactivation is linked to increased vascular permeability [27,28], Thus, further understanding of temporal and stimulus-specific Rac1 activation/inactivation is paramount.

Guanine nucleotide exchange factors (GEFs) serve as Rac activators via promoting the dissociation of GDP from Rac, facilitating GTP binding. Among the large number of GEFs associated with activating Rac1, enriched Dock1 (dedicator of cytokinesis 1) expression was detected in ECs [29] and is critically involved in Rac1-dependent cytoskeletal organization [30,31]. Dock1 forms a complex with Elmo1 through the N-terminal region containing an Src homology (SH)3 domain and a putative-helical region [32]. Mutant mice lacking Dock1 SH3 domain display a defect in myogenesis [33] as similar defects occurred in Dock1 knockout embryos, demonstrating a physiological relevance of Dock1 and Elmo1 interaction. However, Dock1 involvement in TLR4-mediated acute lung injury remains unexplored. In the present study, we demonstrate that Dock1 is markedly downregulated in lung tissues during sepsis/ ventilation-induced lung injury (VILI)-mediated inflammatory lung injury. Either pharmacological inhibition or genetic depletion of Dock1 in pulmonary ECs resulted in significant alterations in regulation of permeability and barrier resistance, modulated the nmMLCK/MLC2 regulation of lamellipodia formation, and exacerbated ROS production during pulmonary vascular inflammation.

2. Materials and methods

2.1. Reagents

Lipopolysaccharides (LPS, *E. coli* 0127:B8 strain) were purchased from Sigma-Aldrich (St. Louis, MO). Human recombinant Nampt (hrNampt) from MBL International (Woburn, MA) was used after validation of NF-κB activation using phospho-IκBα antibody in extracts of primary endothelial cells treated with 1.5 μg/mL of hrNampt. The eNAMPT-neutralizing monoclonal antibody (mAb), ALT-100, was provided by Aqualung Therapeutics Corporation (Tucson, AZ) and previously described [7,11]. Following primary and secondary antibodies were used: Dock1 (cat# 4846S), phosphoplus NF-κB p65/RelA (Ser536) antibody duet (cat# 8214S), phosphoplus p44/42 MAPK (Erk1/2) (Thr202/Tyr204) antibody duet (cat# 8201S), phosphoPlus p38 MAPK (Thr180/Tyr182) antibody duet (cat# 8203S), phosphoplus SAPK/JNK (Thr183/Tyr185) antibody duet (cat# 8206S), Cortactin (cat# 3502S), myc-tag (cat# 2276S), GFP (cat# 2555S), phospho-MLC2 (Thr18/Ser19) (cat# 3674S), and MLC2 (cat# 8505S) from Cell Signaling Technologies (Danvers, MA), Elmo1 (cat# ab2239) from Abcam (Cambridge, MA), NF-κB (cat# PA5-16545) and Nox4 (Cat# PA5-72816) from Invitrogen (Carlsbad, CA), Dock1 (cat# sc-13,163), Dock2 (cat# sc-365,242), and IL-6 (cat# sc-57,315) from Santa Cruz Biotech (Santa Cruz, CA), PBEF/Visfatin biotinylated antibody (cat# BAF4335) from R&D systems, Ultra Streptavidin-HRP (cat #N504) from ThermoFisher Scientific (Waltham, MA), actin-HRP (cat# A3854-200UL) from Sigma-Aldrich (St. Louis, MO), goat anti-mouse HRP (cat# 102646-170) and goat anti-rabbit HRP (cat# 102645-188) from Jackson ImmunoResearch Laboratories, and rabbit anti-goat HRP from Invitrogen (cat# R21459).

2.2. Preclinical ARDS/VILI animal tissues

All animal care procedures and experiments were approved by the Institutional Animal Care and Use Committee (IACUC, protocol # 13-490, University of Arizona). Snap frozen lung tissues were collected from male Yucatan minipigs (17–20 kg, S&S Farms, Ramona, California), Sprague Dawley male rats (300–350 g, Charles River, Wilmington, MA), and C57BL/6J mice (8–12 weeks, Jackson Laboratories, Bar Harbor, ME) after exposure to LPS/VILI. In the porcine model, male Yucatan minipigs were anesthetized with isoflurane followed by IV anesthesia (TIVA) with propofol (5-15 mg/kg/h), ketamine (2-6 mg/kg/h), and midazolam (0.25–0.75 mg/kg/h) and venous (auricular, dorsal pedal) and femoral artery catheters placed. As we reported [7,8], pigs were ventilated on volume assist-control mode (Galileo mechanical ventilator, Hamilton Medical) and continuously monitored for mean arterial pressure, arterial blood gases, pH, pCO_2, pO_2, HCO_3, SpO_2, lactate, heart rate, RR, and end tidal carbon dioxide (ETCO2) (BM5 VET ICU monitoring system). Pigs received IV LPS (25 μg/kg) infused over a 2 h period while receiving 100 % O2. The Vt was then increased from 13 to 20 mL/kg and the RR adjusted to maintain normal ABG values. 2) LPS/VILI rat [7] and mouse [11,34] ARDS models as we previously described. Anesthetized rats and mice were received LPS (0.1 mg/kg) and (after 18 h) mechanically ventilated (4 h room air, Vt 20 mL/kg, RR 70 breaths/min, PEEP 0 cm H_2O) (Advanced Ventilator System for Rodents, SAR-1000, CWE Incorporated, Ardmore, PA). Animals received a humanized mAb neutralizing eNAMPT (ALT-100, 0.4 mg/kg) or PBS intravenously at the end of LPS infusion period, before high tidal volume ventilation exposure [7]. At least three tissue samples obtained from randomly selected animals of treatments were used for immunoblot analyses.

2.3. Endothelial cell (EC) culture, siRNA transfection and viral transduction

Human pulmonary artery endothelial cells (HPAECs) were obtained from (Lonza, Walkersville, MD) and cultured in EBM-2 complete

medium at 37 °C in a humidified atmosphere of 5 % CO_2, 95 % air, with passages 4–6 used for experimentation. HPAECs were transfected with Dock1 or Elmo1 siRNA (100 nM, Horizon Dharmacon, Lafayette, CO) or a non-Targeting pool (cat# D-001810-10-05) using a transfection reagent siPORT*Amine* (cat# AM4052; Ambion, Austin, TX). On-TARGETPlus set of 4 siRNAs are as follow: siDock1-#1 target sequence, GUACCGAGGUUACACGUUA; siDock1-#2 target sequence, GAAAGUCGAUGGUGGUGAA; siDock1-#3 target sequence, UAAAUGAGCAGCUGUACAA; siDock1-#4 target sequence, GGCCCAAGCCUGACUAUUU; siElmo1-#1 target sequence, GGACUGCCCUCAUAUGAAA; siElmo1-#2 target sequence, GAACUCGCUUUCUCCAUCU; siElmo1-#3 target sequence, GCAUUACGGAGACUUAGAA; siElmo1-#4 target sequence, UGACAAGCAUGAGUACUGU; non-Targeting pool, UGGUUUACAUGUCGACUAA, UGGUUUACAUGUUGUGUGA, UGGUUUACAUGUUUUCUGA, GGUUUACAUGUUUUCCUA. For Nrf2 knockdown, short hairpin RNA against human Nrf2 (TRC gene set 7555) was used and compared with TRC lentiviral non-targeting shRNA control (purchased from Dharmacon). Lentiviruses prepared from 293 T cells co-expressing the packaging vectors (psPAX2 and pMD2.G; a gift from Didier Trono/Addgene, Watertown, MA) were used for infection of human lung primary endothelial cells. Human TLR4-expressing HEK293 cells (HEK-Blue-hTLR4; cat# hkb-htlr4, InvivoGen) were used following the manufacturer's instruction.

2.4. Immunoblotting

Immunoblotting to detect proteins in cells, mice, rats, and minipigs tissue homogenates was performed as we have previously reported [7]. Briefly, cells or snap-frozen lung tissues were homogenized in RIPA buffer (50 mmol/L Tris-HCl pH 7.4, 150 mmol/L NaCl, 0.5 % sodium deoxycholate, 0.1 % SDS, 1 % NP-40, 5 mmol/L EDTA) supplemented with complete protease/phosphatase inhibitor cocktail (Cell Signaling, cat # 5872S) using tissue grinder with glass pestles (VWR Cat #26307–606). After centrifugation (15,000 rpm for 20 min at 4 °C), protein concentration of homogenates was determined by Bio-Rad DC protein assay (cat #5000112). Following incubation for 5 min at 90 °C in loading buffer, aliquots containing equal amounts of protein (20–30 μg) were analyzed by electrophoresis using Bolt 4–12 % gradient gel (ThermoFisher Scientific). Subsequently, proteins were transferred to polyvinylidene difluoride (PVDF) membranes and probed with specific primary and appropriate secondary antibodies. Proteins were visualized using a Pierce Western Blotting Substrate (Cat# 32106) or SuperSignal West Pico PLUS Chemiluminescent Substrate (cat #34580) and Chem-iDoc MP imaging system (Bio-Rad). Densitometric analysis was performed using Bio-Rad Image Lab 6.01 software by normalizing the levels of proteins to b-actin expression. The levels of phospho-proteins were quantified by normalizing the levels to their respective total proteins.

2.5. Immunoprecipitation

293 T cells were transfected with pCG.His7.DOCK1 or pCG.myc. ELMO1 plasmids (kindly provided by Dr. Skowronski J., Case Western Reserve University, Cleveland, OH) using Lipofectamine 3000 (cat# L3000015, ThermoFisher Scientific) following the manufacturer's protocol. At 72 h post-transfection, transfectants were lysed in RIPA buffer. Cell lysates were incubated with 1 μg of mouse monoclonal Dock1 antibody and 20 μL of protein A/G magnetic beads (cat# 88803, Pierce) on a rotator at 4 °C overnight. For myc-Elmo1 immunoprecipitation, anti-c-Myc magnetic beads (cat# 88842, Pierce) were used. For GFP-cortactin immunoprecipitation, GFP-trap magnetic beads (cat# gtma20, ChromoTek) were used. The immunoprecipitated complexes were washed with RIPA buffer five times and eluted in sample buffer by boiling for 5 min. Samples were then resolved by SDS-PAGE and subjected to immunoblot analysis.

2.6. Murine plasma IL-6 measurement via the Meso Scale Discovery (MSD) platform

A Meso Scale ELISA-based Discovery Platform was utilized (Meso Scale Diagnostics) for measurements of plasma levels of IL-6 as previously described [12].

2.7. Luciferase assay

Human TLR4-expressing HEK293 (HEK-Blue-hTLR4) cells were maintained as the manufacturer's protocol. The cells were co-transfected with 2.5 μg of pGL3-IL-6 luciferase construct and 0.1 μg of pEF-*Renilla*-luc either with 2.5 μg of Dock1 or Elmo1 plasmid. After 24 h, transfectants were seeded in a 96-well plate and then treated with 0, 0.1 or 1 μg/mL LPS for 16 h. IL-6 luciferase activity (mean ± SD, $n = 3$) was determined by dual luciferase assay [35].

2.8. Rac1-GTP pulldown and G-LISA assay

Rac1-GTP pulldowns were performed using the Active Rac1 Detection Kit purchased from Cell Signaling Technology (cat# 8815) as described by the manufacturer's protocol. Aliquots of the cell extracts or lung tissue homogenates were incubated with the GST-fusion Rac-binding domain of PAK1 at 4 °C for 1 h. The bound proteins and the total extract controls were analyzed by immunoblotting with anti-Rac1 antibody (05–389, Millipore). For measuring Rac1 activation levels, the G-LISA-Rac1 activation assay kit (Cytoskeleton Inc., cat# BK126) was used. Endothelial cells were transfected with indicated siRNAs for 72 h, and then processed following the manufacturer's instructions. Aliquots (1 mg/mL) of tissue lysates were also placed with Rac1-GTP-binding protein linked to the wells of a 96 well plate. Active Rac1 was determined with Rac1 specific antibodies, and the signal is developed with HRP detection reagents following manufacturer's instructions. For the porcine lung tissues, the anti-Rac1 antibody (05–389, Millipore) was used instead of the anti-Rac1 antibody (Cat# ARC03) included in the kit.

2.9. ROS measurements

Human pulmonary endothelial cells were treated at 37 °C with DMSO or TBOPP (10 μM) before stimulation of NAMPT (1.5 μg/mL). After the stimulation for 1 h, CM-H2DCFDA (5 μmol/L; Cat# C6827, ThermoFisher Scientific) was added to each well, incubated at 37 °C for 30 min, and then images were captured using a fluorescence microscope (Olympus CKX53 system) for quantitation of relative fluorescence intensity (RFI).

2.10. Quantitative real-time PCR (qRT-PCR) analysis

Total RNA was extracted from cells by using a Quick-RNA™ Miniprep kit (cat# R1054; Zymo Research, Orange, CA). Equal amounts of total RNA (1 μg RNA) were subjected to first-strand cDNA synthesis using iScript cDNA synthesis kit (cat# 1708891, Bio-Rad) according to the manufacturer's protocol. qRT-PCR reactions with Bio-Rad SsoAdvanced Universal SYBR Green Supermix (cat# 1725272, Bio-Rad) were performed using a Bio-Rad CFX96 Touch System. Predesigned primer sets for each of the following genes were purchased for qRT-PCR analysis of gene expression (purchased from Integrated DNA Technologies, Inc., Coralville, IA): *Dock1, Dock2, Dock3, Dock4, Dock5, Elmo1, ACTINB, and 18S*. For data analysis, raw counts were normalized to the housekeeping gene averaged for the same time point and condition (ΔC_t). Counts are reported as fold change relative to the untreated control ($2^{-\Delta\Delta}C^t$). Following human primers are used: 18S forward, 5'-GTAACCCGTTGAACCCCATT-3′; 18S reverse, 5'-CCATCCAATCGGTAGTAGCG-3′; Dock1 forward, TTTGCGAGCCGTGTTTACTG; Dock1 reverse, ACGCGAACAATCTGACAGAC; Dock2 forward, TGCAGACCGGAAATTTCAGC; Dock2 reverse, AAGGTCGCACTGAAATGCTG; Dock5 forward,

CACCCTCATCTGCTCCACAA; Dock5 reverse, TCTCTCCTCCATCCACTTCCA; Elmo1 forward, CCGGATTGTGCTTGAGAACA; Elmo1 reverse, CTCACTAGGCAACTCGCCCA; IL-6 forward, CCA GAG CTG TGC AGA TGA GT; IL-6 reverse, CTG CAG CCA CTG GTT CTG; IL-1β forward, CCA CAG ACC TTC CAG GAG AAT G; IL-1β reverse, GTG CAG TTC AGT GAT CGT ACA GG. Following mouse primers are used: IL-6 forward, CCC CAA TTT CCA ATG CTC TCC; IL-6 reverse, CGC ACT AGG TTT GCC GAG TA; IL-1β forward, GAA ATG CCA CCT TTT GAC AGT; IL-1β reverse, CTG GAT GCT CTC ATC AGG ACA; ACTINB forward, 5′-AAG GCC AAC CGT GAA AAG AT-3; ACTINB reverse, 5′- GTG GTA CGA CCA GAG GCA TAC-3′.

2.11. Trans-endothelial electrical resistance measurements

Trans-endothelial electrical resistance (TER) across EC monolayers represents changes in paracellular permeability occurred by alteration in cell-cell adhesion. TER measurement was performed by electric cell substrate impedance sensing system (ECIS) (Applied Biophysics, Troy, NY, USA). Human pulmonary artery EC were plated on evaporated gold microelectrodes coated with Collagen I (37 °C, 5 % CO2) at a density of 35,000 cells per well. After overnight culture, cells were pretreated with TBOPP for 2 h and then further treated with S1P, Tysiponate, eNAMPT, LPS or thrombin. TER values were obtained every 3 min for overnight as an automatically recorded resistance (TER = $R_{TER} \times M_{area}$ (cm^2), R_{TER} represents the monolayer cell resistance). The relative TER values were calculated by dividing actual TER values at each time point by the initial TER values (mean ± SEM).

2.12. Statistical analysis

Statistical analysis was performed by one-way ANOVA followed by Bonferroni's *t*-test for multiple comparisons using GraphPad Prism v7.0 (La Jolla, California). Student t-test was used when two groups were compared, and P, 0.05 was regarded as significant.

3. Results

3.1. Dock1 and Elmo1 protein expression are downregulated in lung tissues from preclinical ARDS/VILI animal models

To interrogate the molecular mechanisms underlying the TLR4 permeability responses, we examined the in vivo expression of lung Dock1 and Elmo1 in three complementary preclinical models of human ARDS. Increased production of inflammatory cytokines such as IL-6 and IL-1β in the plasma of ARDS animals were reported previously [7,11,34]. Expression of both Dock1 and Elmo1 proteins was detected in control minipig lung tissue homogenates (Fig. 1A and Supp Fig. S1A), however, lung tissues from LPS/VILI-challenged pigs displayed prominent decreases in Dock1 and Elmo1 protein expression, which were significantly inhibited in animals receiving the eNAMPT-neutralizing ALT-100 mAb [7]. Similar to results in porcine ARDS/VILI lung tissues, examination of Dock1 and Elmo1 expression in LPS/VILI-exposed rats revealed marked loss of lung Dock1 expression and decreased Elmo1 expression (Fig. 1B and Supp Fig. S1B) compared to the control rats. Both Dock1 and Elmo1 expression was again preserved in LPS/VILI-treated rats receiving the eNAMPT-neutralizing mAb. We next examined the time course of TLR4-induced reductions in both lung Dock1 and Elmo1 expression in rats exposed to intratracheal LPS. These studies showed time-dependent decreases in Dock1 and Elmo1 expression beginning at 2 h post LPS challenge (Fig. 1C and Supp Fig. S1C) with near total loss of Dock1 and Elmo1 expression by 4 h post LPS.

Elmo1 interacts with Dock1 to maintain Dock1 protein stability and functionality as a GEF for Rac1 activity [31]. The extent of Rac1 activity in control and ARDS lung tissues was examined by evaluating the activated GTP-bound state and inactive GDP-bound state via GTPase pull-down assays. These studies demonstrated that LPS/VILI-treated porcine lungs exhibit a ~ 40 % reduction in activated GTP-bound Rac1 compared to control lung tissues (Fig. 1D, Supp Fig. 1D) without significant alterations in total Rac1 levels. Consistent results were also obtained from a G-LISA specific for Rac1 utilizing a luminescent readout (Fig. 1D, right). Similarly, LPS/VILI-treated rat lung tissues exhibited ~45 % lowering of GTP-bound Rac1 levels (Fig. 1E; Supp Fig. 1E), with both porcine- and rat-activated GTP-bound Rac1 levels nearly normalized in animals receiving the eNAMPT ALT-100 mAb. These studies indicate TLR4 activation (either by LPS or eNAMPT) downregulates Dock1-Rac1 activity in concert with the induction of the inflammatory lung response. As we and others have shown that Rac1 inactivation is linked to increased vascular permeability [27,28], the marked loss of Dock1 expression and reduced Rac1 activity appears to contribute to the severity of preclinical ARDS/VILI pathobiology.

Elmo1-Dock1 interaction prevents proteasomal protein degradation. To verify direct Dock1 and Elmo1 interaction, his-tagged Dock1 and

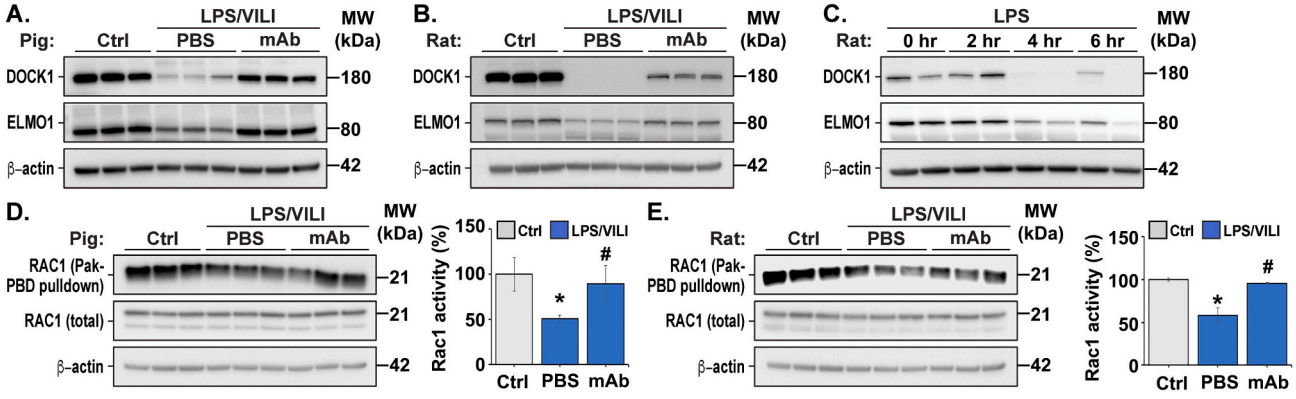

Fig. 1. Expression of Dock1 and Elmo1 is decreased in preclinical models of ARDS/VILI-mediated inflammatory lung injury. A. Septic shock/VILI-challenged Yucatan minipigs received placebo (PBS; $n = 3$) or eNAMPT-neutralizing mAb (n = 3) 2 h after onset of injury as outlined in the Methods. Lung tissues isolated from these pigs and untreated control pigs (Ctrl; n = 3) were homogenized for immunoblotting analysis of Dock1 and Elmo1 expression. B. Dock1 and Elmo1 expression was examined by immunoblotting analysis in lung homogenates of rats receiving either placebo (lanes 4–6, PBS; n = 3) or eNAMPT-neutralizing mAb (lanes 7–9, mAb; n = 3) followed by LPS/VILI and compared to control rats (lanes 1–3, Ctrl; n = 3). C. Representative lung immunoblots of Dock1 and Elmo1 expression in rat LPS-challenged rats (intratracheal LPS, 1 mg/kg) in a time course (duplicate). D/E. In pig (D) and rat (E) lung tissues, active Rac1 was isolated with PAK-GST beads. Isolated complexes were separated by Immunoblotting and probed with anti-Rac antibodies (n = 3). Tissue homogenates were probed in parallel to monitor total cellular Rac1 levels. Changes in Rac1 activity assessed by a G-GLISA are expressed in percentages of control (Ctrl) values, and each bar graph represents the mean ± SD of triplicate. *$p < 0.05$, LPS/VILI+PBS vs. Ctrl; #$p < 0.05$, LPS/VILI+mAb vs. LPS/VILI+PBS.

myc-tagged Elmo1 were transiently co-transfected into 293T cells, and myc-tagged Elmo1 immunoprecipitated from whole cell lysates. Immunoblotting studies confirmed the Dock1 and Elmo1 presence within myc-Elmo1 immunoprecipitates, indicating a direct interaction between Dock1 and Elmo1 proteins in the absence of cell stimulation with EGF (Supp Fig. S2A). These data further showed that elevated Elmo1 expression increases the direct Elmo1 interaction with cortactin, an important actin-binding protein and regulator of EC junctional integrity and barrier function [36,37]. The binding of cortactin and Elmo1 was further verified by co-immunoprecipitation of GFP-cortactin and myc-Elmo1 in co-transfected cells (Supp Fig. S2B). Dock1 and Elmo1 interaction was next examined in human pulmonary ECs with Dock1 protein immunoprecipitation studies demonstrating endogenous Dock1 interaction with Elmo1 (Fig. 2A) was not influenced by either LPS or thrombin stimulation. To better understand the role of Dock1 and Elmo1 in lung EC barrier integrity, the *Dock1* gene was silenced utilizing the most effective small interference RNA (siRNA), siRNA1 (compared to siRNA2, siRNA3, siRNA4) and siRNA2 utilized for *Elmo1* gene silencing (among 4 sets of Elmo1 siRNAs) (Supp Fig. S3A/S3B). Functional activity of the selected siRNAs against Dock1 or Elmo1 was evaluated by the G-LISA-Rac1 assay. Knockdown of either Dock1 or Elmo1 resulted in reduced Rac1 activity in ECs (Supp Fig. S3C). siRNA-mediated knockdown of Dock1 or Elmo1 expression in ECs (qRT-PCR and immunoblot validation) showed that reduced Dock1 expression does not affect Elmo1 gene expression, whereas siElmo1 transfection downregulated Dock1 protein expression without altering Dock1 mRNA levels (Fig. 2, B, C, and Supp Fig. S3D). EC treatment with the proteasome inhibitor, MG132, failed to increase Dock1 or Elmo1 expression (Supp Fig. S3E). In the siElmo1 transfectants, however, MG132 treatment increased Dock1 protein levels (Fig. 2, D/E), indicating that the loss of Elmo1 increases proteasomal degradation of Dock1, a potential explanation for the marked loss of Dock1 protein observed in preclinical ARDS/VILI lung tissues (Fig. 1).

3.2. *Dock1 inhibition augments eNAMPT/TLR4-induced vascular permeability*

eNAMPT/TLR4 inflammatory signaling results in disruption of lung EC monolayer integrity and significant increases in lung vascular permeability [38]. Given the observed preservation of Dock1 protein levels in lung tissues from eNAMPT ALT-100 mAb-treated ARDS/VILI animals, we examined whether Dock1 inhibition augments the capacity for eNAMPT/TLR4 to increase EC permeability assessed by changes in trans-endothelial electrical resistance (TER), a highly sensitive in vitro measure of EC permeability measured by electric cell substrate impedance sensing system (ECIS). EC grown on the gold microelectrodes and exposed to the TLR4 agonists, eNAMPT and LPS, displayed significantly increased EC barrier disruption, which was amplified in lung EC pre-incubated with the Dock1 inhibitor, TBOPP (Fig. 3, A/B). TBOPP-mediated Dock1 inhibition also significantly augmented thrombin-induced EC barrier disruption (Fig. 3C). TySIPonate (TyS1P), a sphingosine 1-phosphate (S1P)-related analog and potent EC barrier-enhancing agent [39–41], induced robust EC barrier enhancement which was significantly inhibited by Dock1 inhibition (Fig. 3D). These data indicate Dock1 is a direct and important contributor to EC barrier integrity and barrier preservation.

3.3. *Involvement of eNAMPT/TLR4 and DOCK1 in redox dysregulation in vitro and preclinical ARDS/VILI models*

To decipher the mechanism for augmented eNAMPT/TLR4-mediated barrier disruption by Dock1 inhibition, we examined the expression of the ROS-producing Nox4 and the ROS-sensing transcription factor, Nrf2. We and others have previously shown Nox4 and Nrf2 to be important factors in regulating EC barrier integrity [2,24]. EC exposure to eNAMPT or the Dock1 inhibitor TBOPP increased Nox4 expression (Fig. 4A and Supp Fig. S4A), confirmed by Dock1 silencing (Fig. 4B and Supp Fig. S4B). While phospho-IκBα (NF-kB activation) levels were increased in ECs treated with eNAMPT and TBOPP, the increase of phospho-TBK1 (TLR4 activation) was specific to eNAMPT. Predictably, Elmo1 silencing reduced Dock1 expression and induced Nox4 upregulation, suggesting that Dock1 inhibition may increase ROS production via Nox4 upregulation. qRT-PCR analysis further showed that Dock1 silencing resulted in reduced *Nrf2* gene expression and reduced expression of key Nrf2 transcriptional targets, heme oxygenase 1 (*Hmox1*) and NAD(*P*)H quinone dehydrogenase 1 (*Nqo1*) (Fig. 4C). Similar findings were observed with EC exposed to the Dock1 inhibitor, TBOPP, with slightly reduced Nrf2 and Hmox1 protein expression and augmented eNAMPT-

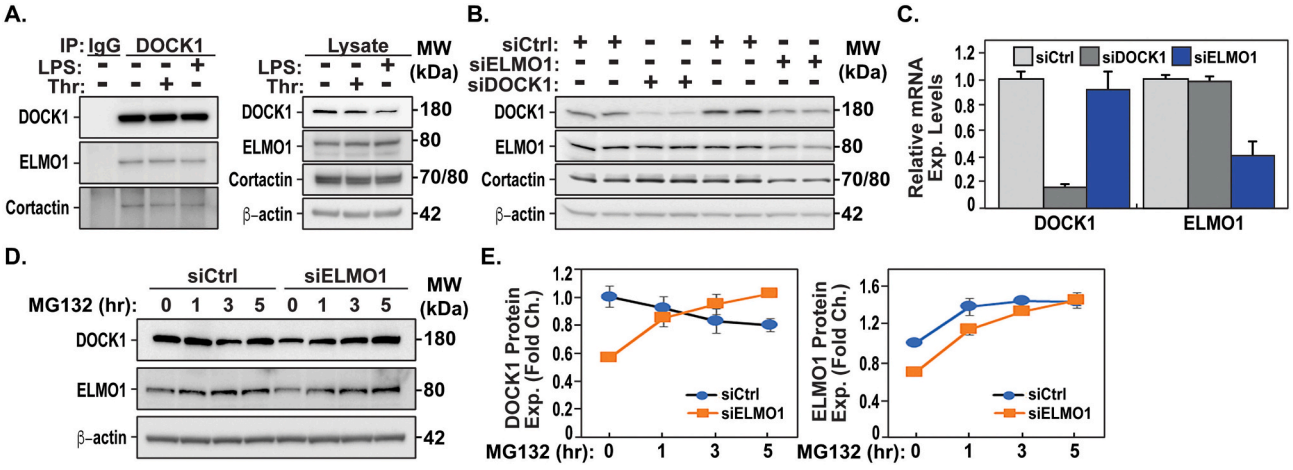

Fig. 2. Reduced Elmo1 expression promotes Dock1 protein degradation. A. Human pulmonary artery endothelial cells (ECs) were treated with LPS or Thrombin (Thr) for 1 h (hr). Total cellular lysates were subjected to IgG or Dock1 immunoprecipitation (IP) and analyzed by immunoblotting with the indicated antibodies. B. ECs were transfected with siCtrl, siDock1, or siElmo1. After 72 h transfection, silencing effects of each siRNAs were analyzed by immunoblotting with the indicated antibodies (two sets of independently prepared samples). C. qRT-PCR was performed for Dock1 and Elmo1 mRNA expression after transfection of siCtrl, siDock1, or siElmo1. Data shown were generated from two sets of independently prepared samples assessed by qRT-PCR twice. Target gene expression was normalized to 18S levels. *$p < 0.05$, siDock1 (or siElmo1) vs siCtrl. D. Immunoblot analysis of Dock1 accumulation after MG132 treatment. ECs were transfected with siCtrl or siElmo1. After 24 h, these transfectants were exposed to 10 μmol/L MG132 for the indicated time. Total cell lysates were subjected to immunoblot analysis. E. Dock1 and Elmo1 protein expression was determined by densitometry and the levels of Dock1 and Elmo1 relative to those of actin was plotted as fold changes from untreated control (0 h).

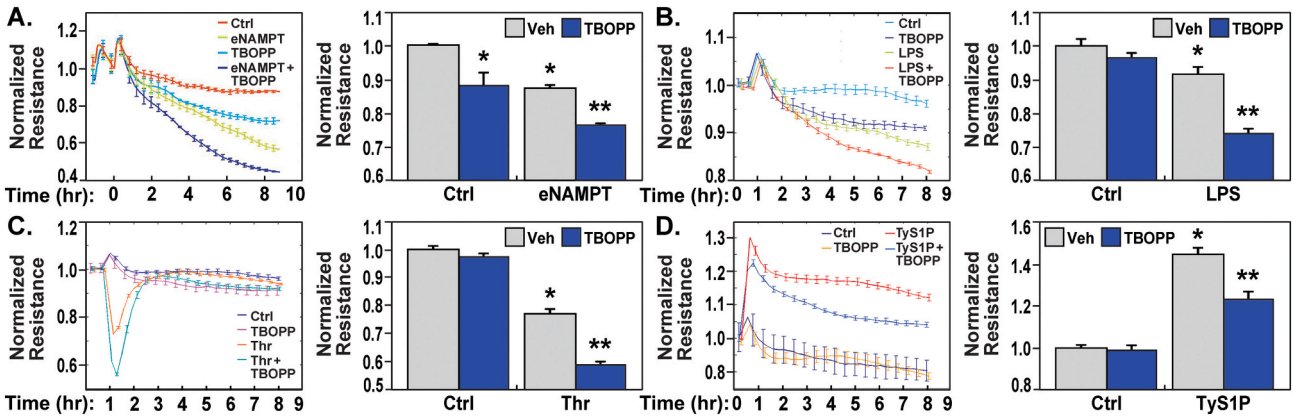

Fig. 3. Inhibition of Dock1 activation of Rac GTPase increases EC barrier dysfunction. EC barrier function was assessed by measurements of trans-endothelial electrical resistance (TER). ECs were pretreated with TBOPP (50 μmol/L for A, 25 μmol/L for B—D) for 2 h followed by challenge with eNAMPT (1.5 μg/mL, A), LPS (1 μg/mL, B), thrombin (0.5-unit, C), and Tysiponate (tyS1P; 1 μg/mL, D). TER was recorded continuously for 8 h to 24 h. Shown graphs are representative tracings from four experiments (mean ± SEM). *$p < 0.05$, treatment vs. ctrl; **$p < 0.05$, single treatment vs. combo.

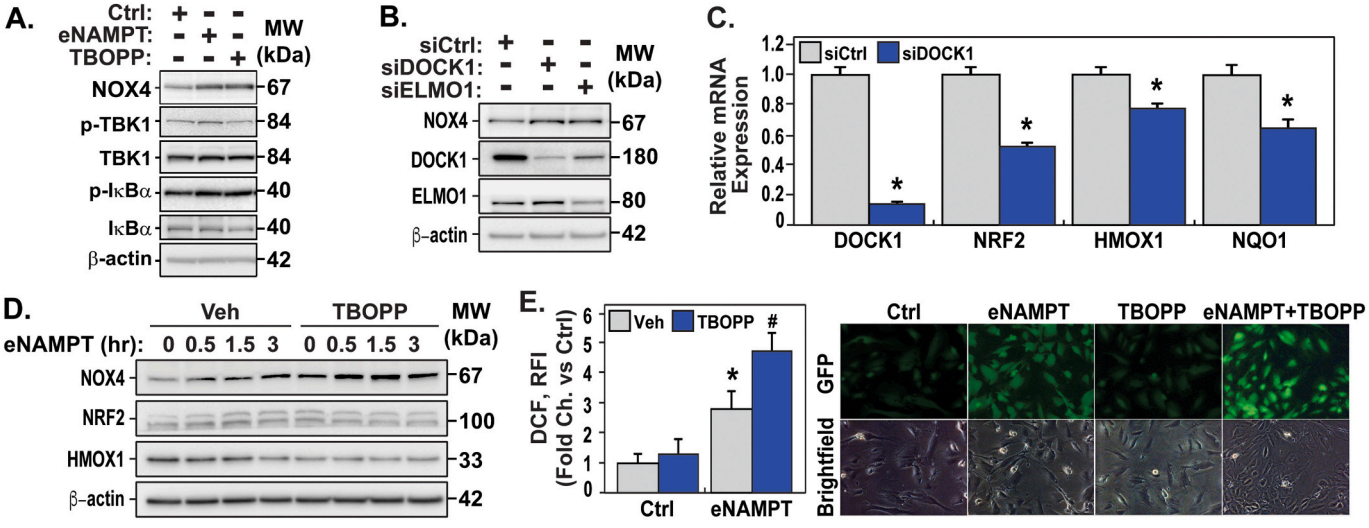

Fig. 4. eNAMPT-mediated ROS generation is augmented by Dock1 inhibition in lung endothelial cells. A. Immunoblot analysis of Nox4 expression. ECs were treated with 1.5 μg/mL rhNAMPT (3 h) and 10 umol/LTBOPP (16 h) Total cell lysates were subjected to immunoblot analysis as the indicated antibodies. B. ECs were transfected with siCtrl, siDock1 or siElmo1. After 72 h, Nox4 expression in these transfectants were determined by immunoblotting analysis. C. Effects of siRNA Dock1 (siDock1) on Nrf2, Hmox1 and Nqo1. Human lung ECs were transfected with siCtrl or siDock1. After 72 h transfection, total RNA extracts were used for qRT-PCR analysis. Normalized fold expression of Nrf2, Hmox1 and Nqo1 mRNA (duplicate) is shown and 18S was used for normalization. D. Immunoblots of Nox4, Nrf2 and Hmox1 expression. ECs were pretreated for 16 h with DMSO or 10 μM TBOPP and further treated with rhNAMPT for the indicated times. E. ROS measurement. Relative fluorescent intensity (RFI) was counted after dichlorofluorescein (DCF) staining of ECs after rhNAMPT, TBOPP and the combination of rhNAMPT and TBOPP and then stained for 0.5 h with 5 umol/L CM-H2DCFDA. Data are shown as mean ± SEM of triplicates. Scale-500 μm. *$p < 0.05$, treatment vs. Ctrl; #$p < 0.05$, eNAMPT vs. combo.

mediated Nox4 upregulation (Fig. 4D and Supp Fig. S4C). EC staining with H_2DCF-DA to visualized ROS levels demonstrated both eNAMPT and TBOPP to augment ROS production (Fig. 4E). These results indicate that eNAMPT/TLR4-mediated impairment of EC redox regulation [7] may involve reduced Dock1 expression resulting in Nox4 upregulation and reduced Nrf2 expression and transcription targets.

To gain an insight whether Dock1 can regulate inflammatory signaling, we silenced Dock1 expression in ECs and measured IL-6 and IL-1β mRNA expression by qRT-PCR and demonstrated that both cytokine genes were significantly induced by Dock1 silencing (Fig. 5A). We also co-transfected Dock1 and IL-6 luciferase reporter plasmids into hTLR4-overexpressing HEK293 cells. After LPS treatment, control transfectant showed marked increases in IL-6 luciferase activity, however, overexpression of Dock1 or Elmo1 significantly lowered the LPS-induced IL-6 luciferase activity (Fig. 5B). We next sought to determine whether oxidative stress regulated by Dock1 contributes to inflammatory lung injury employing a mouse LPS/VILI model, with significant increases in plasma IL-6 and IL1β expression (Fig. 5C). qRT-PCR analysis of mouse lung tissues to examine a potential inverse relationship between lung Dock1-Elmo1 and the two inflammatory cytokines, identified IL-6 and IL-1β mRNA expression to be significantly increased in lung tissues of LPS/VILI mice compared to controls (Fig. 5D). In contrast, both Dock1 and Elmo1 mRNA were significantly downregulated in the lung tissues of LPS/VILI mice. Immunoblotting analysis of lung tissue homogenates from mice exposed to LPS/VILI showed increased NF-κB, ERK and JNK activation and levels of IL-6 and NAMPT expression compared to control mice (Fig. 5E/5F, Supp Fig. S5A/S5B). Notably, LPS/VILI-altered lung tissue redox states, reflected by increased Nox4 expression and decreased Nrf2 expression, coincided with down-regulated Dock1 and Elmo1 lung tissue expression (Fig. 5F and Supp

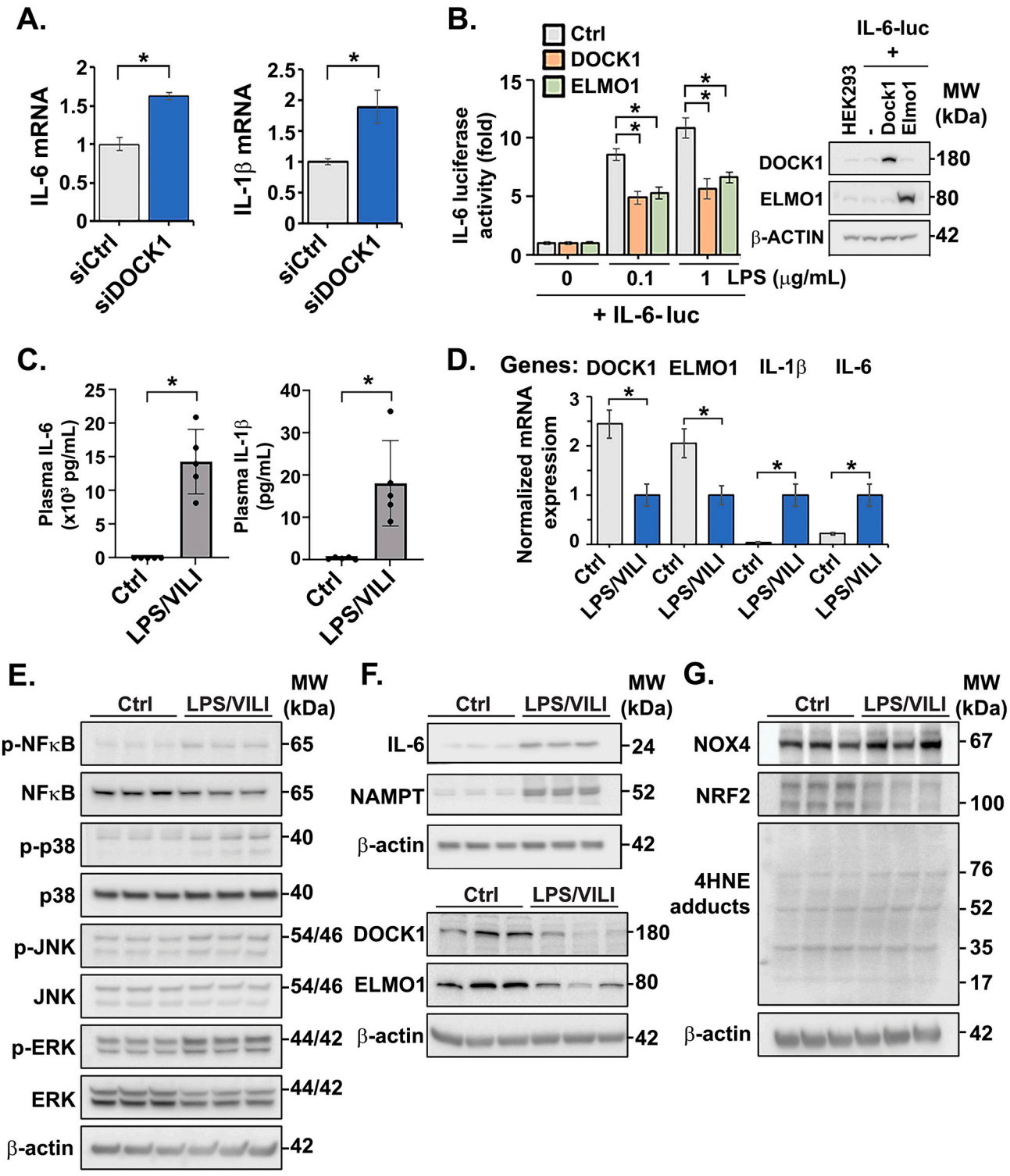

Fig. 5. Impaired redox regulation and inflammatory signaling is linked to loss of Dock1 expression in preclinical mouse ARDS lung tissues. A. qRT-PCR analysis of IL-6 and IL-1β mRNA expression. ECs were transfected with siCtrl or siDock1 for 72 h. *$p < 0.05$, siCtrl vs. siDock1 (mean +/− SD, $n = 4$). B. hTLR4-HEK-293T cells were cotransfected with IL-6-luc, renilla-luc and Dock1 (or Elmo1) plasmids with immunoblot detection of Dock1 and Elmo1 overexpression in these transfectants (right panel). IL-6 luciferase activity was increased by LPS challenge (16 h, mean+/-SD, $n = 3$) but reduced in Dock1 and Elmo1 silenced cells. C. Plasma levels of IL-6 and IL-1β measured by MesoScale Discovery platform were markedly increased in LPS/VILI-challenged mice. *$p < 0.05$, Ctrl vs. LPS/VIL (mean +/− SD, $n = 5$). D. qRT-PCR analysis of mouse lung IL-6 and IL-1β, Dock1 and Elmo1 mRNA expression. *$p < 0.05$, Ctrl vs. LPS/VILI (mean ± SD, n = 5). E. Lung tissue homogenates were obtained from mice exposed to LPS/VILI and from untreated control mice. Representative immunoblotting images of phosphorylated proteins of NF-kB (p-NF-κB), JNK (p-JNK), p38 (p-p38), ERK (p-ERK). F. Similarly, IL-6, NAMPT, Dock1 and Elmo1 protein expression in mouse lung tissues was increased in ARDS/VILI-challenged animals (representative immunoblot shown). G. Expression of 4-Hydroxynonenal (4-HNE) adduct formation, Nox4 and Nrf2 in the lung tissues of mice challenged with LPS/VILI and controls was assessed by immunoblot analysis.

Fig. S5C). We also identified increased lipid peroxidation products, 4-HNE adducts, in LPS/VILI-challenged mouse lung tissues compared with controls (76 kDa and 52 kDa proteins, Fig. 5G and Supp Fig. S5D), reflecting ROS- induced oxidative tissue damage [42,43]. Together, these results suggest that ARDS/VILI-induced increases in ROS reflect the contribution of eNAMPT/TLR4-induced redox dysregulation, NOX4 expression, and loss of Dock1 expression.

3.4. Dock1 is required for S1PR1-mediated EC MLC2 phosphorylation

EC barrier regulation involves a highly dynamic balance between barrier-disrupting cellular contractile forces and barrier-protective tethering forces, with both competing forces linked to the EC actin cytoskeleton [44]. S1P receptor 1 (S1PR1) ligation elicits a EC signaling cascade that enhances the formation of a cortical actin ring, improves cell-cell and cell-matrix interactions, and increases EC barrier function in vitro [45] and in vivo [46]. Myosin light chain 2 phosphorylation catalyzed by nmMLCK at serine-19 and threonine-18 drives actomyosin interaction, contractility, cell migration, and endo/exocytic processes [47,48], and is recognized for its key role in regulating spatially-specific cell–cell adhesion and EC barrier function [49]. To examine Dock1 involvement in EC cytoskeletal dynamics, ECs were treated with TBOPP, stimulated with S1P, and levels of MLC phosphorylation measured. S1P induced robust MLC2 phosphorylation in ECs at 5 min exposure (Fig. 6A and Supp Fig. S6A) as previously reported [24,45] with TBOPP pre-treatment mildly reducing basal levels of MLC phosphorylation and abrogating S1P-mediated MLC2 phosphorylation (Fig. 6A). Dock1 silencing siRNAs exerted similar findings (Fig. 6B, Supp Fig. S6B). Elmo1 depleted (siRNA) ECs, with reduced Dock1 expression, also exhibited attenuated S1P-induced MLC2 phosphorylation. Consistent with changes in MLC2 phosphorylation, nmMLCK tyrosine phosphorylation, an indicator of kinase activation, was also increased by S1P exposure but inhibited by both TBOPP and siDock1 (Fig. 6C/D, Supp Fig. S6C/S6D).

Next, we infected ECs with lentiviruses of shNrf2 to explore disrupted redox balance as a mechanism for regulation of nmMLCK/MLC signaling by Dock1 inhibition. Reduced Nrf2 expression significantly altered redox regulation, reflected by the marked downregulation of Hmox1 expression. S1P was ineffective in increasing nmMLCK or MLC2 protein phosphorylation in shNrf2-treated ECs compared to shControl-ECs (Fig. 6E, Supp Fig. S6E). In addition to its pivotal role in driving actin polymerization, nmMLCK-mediated MLC phosphorylation is critical to EC barrier-enhancing lamellipodia formation after S1P challenge. It colocalizes with cortactin and actin in the cell periphery and lamellipodia [25,41]. We assessed Dock1 involvement in lamellipodia formation in ECs treated with S1P, TyS1P, or HGF in the presence or absence of TBOPP (Fig. 6F). These studies showed that TBOPP significantly abrogated S1P- or TySIP-mediated cortactin/actin peripheral colocalization in peripheral edges of cells compared to control or HGF-treated cells formation (Fig. 6F), again indicating that EC barrier-enhancing responses involve lamellipodia appearance, which is dependent on Dock1 activity.

4. Discussion

Activation of the evolutionarily-conserved TLR4 inflammatory cascade results in profound inflammatory alveolar edema and is a major contributor to the excess mortality observed in subjects with ARDS and in COVID-infected individuals. Our previous works using the highly relevant mouse, rat, and porcine preclinical models of ARDS/VILI demonstrated that in addition to LPS-mediated activation of the pathogen recognition TLR4 receptor, TLR4 signaling elicited by the novel DAMP, eNAMPT, is also a key contributor to the severity of inflammatory lung injury [11] [50]. The current study was designed to mechanistically explore the role of Dock1/Elmo1 and Rac GTPase in the dysregulated inflammatory permeability responses following TLR4 ligation. Although the Dock1-Elmo1 complex is a critical regulator of

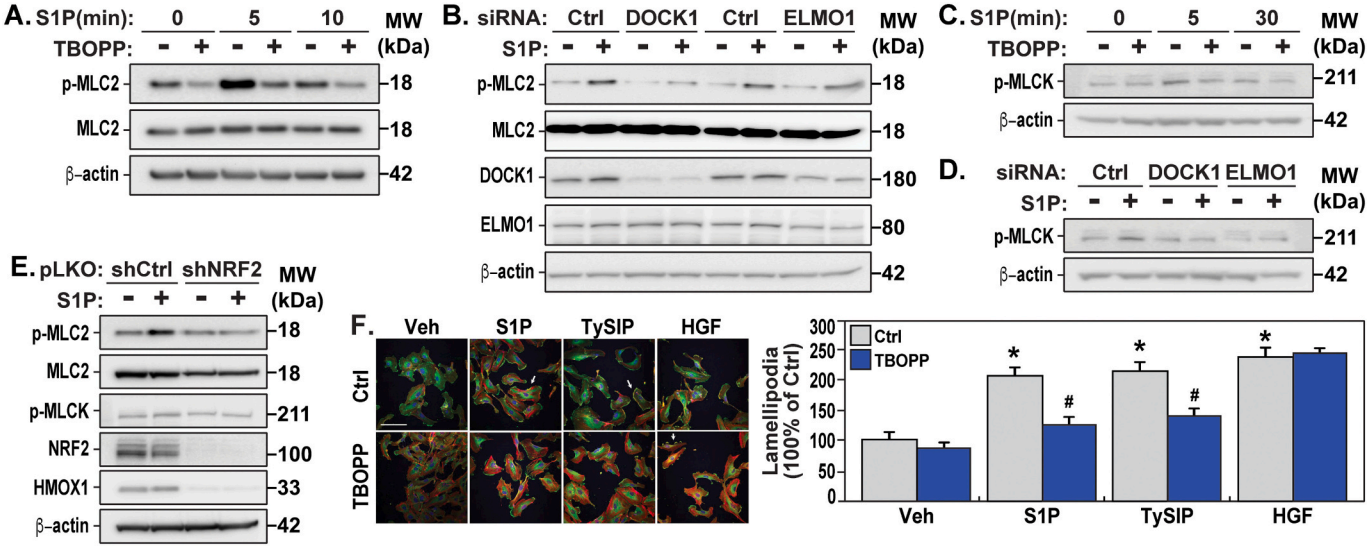

Fig. 6. Dock1 inhibition impairs nmMLCK/MLC2-regulated lamellipodia formation.
A. Human pulmonary artery endothelial cells (ECs) were pretreated with TBOPP (10 μmol/L) and then exposed to S1P (1 μmol/L) for the indicated time. Total cell lysates were used for immunoblotting analysis of phsopho-MLC2 (p-MLC2), total MLC2 and b-actin protein expression. B. ECs were transfected with non-specific scrambled sequence (siCtrl), siDock1 or siElmo1. At 72 h post transfection, transfectants were exposed to S1P (1 μmol/L) for 5 min. Total cell lysates were used for immunoblotting analysis with the indicated antibodies. C. Immunoblot of phospho-MLC kinase (p-MLCK) is shown. β-Actin was used as a loading control. Preparation of samples are described for Panel A. D. Changes in p-MLCK expression are shown with or without S1P exposure (1 μmol/L, 5 min) in ECs after 72 h post-transfection with siCtrl, siDock1 or siElmo1. β-actin was used as a loading control. E. Immunoblot analysis of phospho-MLC kinase and MLC2 expression after S1P exposure of Nrf2-depleted ECs. ECs were infected with lentiviruses of shControl (shCtrl) or shNrf2. After 7 days, shCtrl and shNrf2 transduced ECs were exposed to S1P (1 μmol/L) for 5 min. Immunoblotting studies confirmed that shNrf2 transduction depleted Nrf2 and its transcriptional target Hmox1 expression. F. Lamellipodia formation in ECs. HPAECs in chamber slides were pre-treated for 1 h with 10 μmol/L TBOPP, a specific DOCK1 inhibitor, before exposing them to S1P (5 μmol/L), TySIPonate (2 μM) or HFG (20 ng/mL) for 1 h. Cells were formalin-fixed, permeabilized and stained with mouse anti-cortactin(green) and phalloidin (red). Arrow indicates lamellipodiae; Scale-40 μm. $^{*}p < 0.05$, treatment vs. Ctrl; $^{\#}p < 0.05$, combo vs single treatment.

Rac GTPase, the involvement of Dock1-Elmo1 in influencing the severity of inflammatory lung injury in preclinical ARDS/VILI models has not been previously addressed. In this study, we highlight the involvement of marked dysregulation of Dock1 and Elmo1 expression in inflammatory lung injury, which was preserved in animals receiving an eNAMPT-neutralizing mAb. Dock1 and Elmo1 lung expression levels were reduced time-dependent following LPS/TLR4 activation, consistent with the tight association of these events with the progression of inflammatory lung injury. We determined that Dock1 is highly expressed in lung EC and tightly complexed with Elmo1 protein, an interaction not disrupted by LPS or mechanical stress. Reduced Elmo1 expression (RNAi), however, increases proteasome-dependent Dock1 degradation suggesting that Elmo1 constrains auto-ubiquitination of Dock1 protein. Although the exact regulation of Elmo1 expression in lung ECs is unknown, we suspect that Elmo1 is ubiquitously expressed since Elmo1 is known to involve in cytoskeletal rearrangements for phagocytosis of apoptotic cells and cell motility [51]. Therefore, decreasing Elmo1 expression is responsible for Dock1 loss in inflammatory lung tissues.

As Elmo1 acts in association with Dock1 to activate Rac GTPase, we examined Rac1 activity in preclinical ARDS/VILI lung tissues with both ARDS/VILI-exposed porcine and rat lungs showing reduced Rac1 activity compared to controls. As the level of Rac1 activity, the reduction was less dramatic compared to the marked losses of Dock1 and Elmo1 in LPS/VILI-treated lungs. Factors other than Dock1-Elmo1 may also contribute to Rac1 activity in inflamed lung tissues. Rac1 activity, like the expression of Dock1 and Elmo1, was preserved in ALT-100 mAb-treated animal groups underscoring the importance of the eNAMPT/TLR4 pathway in evoking Dock1/Elmo/Rac1 dysregulation. We sought to explore a potential mechanism by which the loss of Dock1 expression contributes to TLR4-mediated inflammatory permeability and EC barrier integrity using genetic and pharmacological inhibitor approaches. The Dock1 inhibitor TBOPP blocks the association of the DOCK1 DHR-2 domain with Rac1, abrogating Rac1 activity without affecting cellular functions of the closely related Rac GEFs DOCK2 and DOCK5 [52]. Our in vitro studies determined that pharmacologic inhibition of Dock1 activity (TBOPP) significantly exacerbates the TLR4 agonist-induced loss of EC barrier integrity (LPS, eNAMPT). Dock1 inhibition also attenuates EC barrier-enhancement by S1PR ligands (sphingosine-1-phosphate, Tysiponate) and suppresses the formation of EC barrier-enhancing lamellipodia and nmMLCK-mediated MLC2 phosphorylation. Our siRNA approach for Dock1 gene silencing replicated the inhibitory effects of TBOPP on nmMLCK-MLCK2 phosphorylation stimulated by S1P, again consistent with the involvement of Dock1-Rac1 signaling in EC barrier regulation,

Inflammation-mediated increases in ROS production/oxidative stress are exaggerated when antioxidant defense mechanisms are impaired [53–56], such as with reduced levels of NF-E2-related factor 2 (Nrf2), which binds to antioxidant response elements (AREs) on antioxidant genes [19]. Pharmacological activation of Nrf2 mitigates the severity of ARDS [57,58] and VILI [59], and Nrf2-deficient ($Nrf2^{-/-}$) mice are more susceptible to ARDS stimuli (such as hyperoxia and VILI) compared to wild-type ($Nrf2^{+/+}$) mice [60,61]. Excessive oxidative stress augments lung dysfunction and impairs vascular barrier integrity with the ROS-generating enzyme, NADPH oxidase (Nox4), a critical mediator of inflammatory lung injury in preclinical models of ARDS/VILI [17,62–65]. In vivo silencing of Nox4 expression lowered ROS production in response to LPS and improved survival rate in septic mice. However, the mechanism for Nox4 upregulation and enhanced ROS production in ARDS leads to severe EC barrier dysfunction remains poorly understood. Our work suggests that the influence of Dock1 inhibition on eNAMPT-induced EC barrier disruption involves upregulation of Nox4 expression and reduced expression of Nrf2-mediated ROS scavengers which together result in elevated levels of ROS, critical factors increasing EC barrier disruption. Consistent with the results in ECs, the mouse ARDS/VILI model showed that marked decreases in Nrf2 expression and increases in Nox4 expression are correlated with Dock1 loss in the lung tissues of mice with inflammatory lung injury. Nox4 and Nrf2 are attractive redox regulatory targets to mitigate the severity of ARDS [57,58]. We have also shown that sepsis survival rates are substantially improved by Nox4 knockdown with attenuated lung ROS production in septic mice and attenuated redox-sensitive activation of the nmMLCK pathway, resulting in restored EC tight junctional integrity. The present data indicated that prolonged inhibition of Dock1 activity or loss of Dock1 expression could contribute to deregulated redox status by upregulating Nox4 and lowering Nrf2 expression, thereby leading to impairment of EC barrier regulation.

Dock family proteins regulate actin remodeling by recruiting the actin nucleating-promoting factor Wasf1 through the DHR-1 domain of Dock protein. As spatial activation of Rac1 is needed for the formation of a cortical actin ring [66], we evaluated the effects of Dock1 on nmMLCK-mediated MLC2 phosphorylation that has previously shown to be critically involved in leukocyte influx into lung tissues via cytoskeletal rearrangement and regulation of vascular integrity [2,24]. In response to EC barrier-enhancing signals (S1P, TysSIP), nmMLCK phosphorylates MLC2 protein resulting in lamellipodia formation through actin polymerization in ECs [25]. Our data indicated that Dock1 depletion blocks the S1P-mediated phosphorylation of nmMLCK-MLC2 protein. Inhibitory effects of TBOPP on the MLCK-MLC2 activity were recapitulated by siRNA-mediated Dock1 depletion, consistent with the importance of Rac1 activity on nmMLCK signal transduction mechanism and S1P-mediated EC actin rearrangement and barrier regulation [45].

5. Conclusions

Together, our data indicate that the loss of Dock1 expression during ARDS/VILI inflammatory lung injury significantly contributes to the disruption of EC barrier integrity and exacerbates TLR4-mediated EC barrier permeability. Dysregulated redox signaling and ROS generation mediated by upregulated Nox4 expression and downregulated Nrf2 expression is influenced by Dock1 and implicated in TLR4-induced EC barrier disruption. As lamellipodia formation and MLC2 kinase activity stimulated by S1P/TyS1P was completely inhibited by Dock1 inhibition, our data indicate an important role of Dock1-Rac1 signaling in actin reorganization. Loss of Dock1 expression drives the severity of inflammatory lung injury, so therapeutic strategies to restore Dock1 expression directly may be of significant utility in ARDS/VILI.

Abbreviations

4-HNE	4-Hydroxynonenal
ARDS	acute respiratory distress syndrome
ARE	the antioxidant response element
Dock1	dedicator of cytokinesis 1
EC	endothelial cells
ECIS	electric cell substrate impedance sensing system
GEF	guanine nucleotide exchange factor
Hmox1	heme oxygenase 1
LPS	liposaccharide
mAb	monoclonal antibody
MLC2	Myosin light chain 2
eNAMPT	extracellular nicotinamide phosphoribosyltransferase
NOX4	NADPH oxidase 4
NQO1	NAD(*P*)H Quinone Dehydrogenase 1
Nrf2	NF-E2-related factor 2
rhNAMPT	recombinant human NAMPT
siRNA	small interference RNA
shRNA	small hairpin RNA
TLR4	Toll-like receptor 4
VILI	ventilator-induced lung injury

CRediT authorship contribution statement

JHS, JGNG - Substantial contributions to the conception, design of the work, and writing manuscript. JHS, JBM, SS, CLK, HC, SMC, TB, DDZ, VN, JGNG - the acquisition, analysis, visualization, or interpretation of data contained in this work. JHS and JGNG verified the underlying data, revised critically for important intellectual content and were major contributor in reviewing the entire manuscript. All authors had full access to all the data, provided final approval of the submitted version and agreed to be accountable for all aspects of the work.

Data sharing statement

Data contained within the article and Supplementary materials are publicly available. The all blots of original, uncropped and unadjusted images are available to reader in the supplementary data.

Funding

This work was supported by NIH/NHLBI grants: P01 HL126609, R01 HL094394, R01 HL141387, and P01 HL134610.

Declaration of competing interest

Joe GN Garcia, MD is CEO and founder of Aqualung Therapeutics Corporation. All other authors declare no competing financial interests.

Data availability

Data will be made available on request.

Appendix A. Supplementary data

Supplementary data to this article can be found online at https://doi.org/10.1016/j.bbadis.2022.166562.

References

[1] M.A. Matthay, L.B. Ware, G.A. Zimmerman, The acute respiratory distress syndrome, J. Clin. Invest. 122 (2012) 2731–2740.
[2] S.M. Dudek, J.G. Garcia, Cytoskeletal regulation of pulmonary vascular permeability, J. Appl. Physiol. 91 (2001) (1985) 1487–1500.
[3] B.T. Thompson, R.C. Chambers, K.D. Liu, Acute respiratory distress syndrome, N. Engl. J. Med. 377 (2017) 562–572.
[4] S.B. Hong, Y. Huang, L. Moreno-Vinasco, S. Sammani, J. Moitra, J.W. Barnard, S. F. Ma, T. Mirzapoiazova, C. Evenoski, R.R. Reeves, E.T. Chiang, G.D. Lang, A. N. Husain, S.M. Dudek, J.R. Jacobson, S.Q. Ye, Y.A. Lussier, J.G. Garcia, Essential role of pre-B-cell colony enhancing factor in ventilator-induced lung injury, Am. J. Respir. Crit. Care Med. 178 (2008) 605–617.
[5] E.K. Bajwa, C.L. Yu, M.N. Gong, B.T. Thompson, D.C. Christiani, Pre-B-cell colony-enhancing factor gene polymorphisms and risk of acute respiratory distress syndrome, Crit. Care Med. 35 (2007) 1290–1295.
[6] S. Etienne-Manneville, A. Hall, Rho GTPases in cell biology, Nature 420 (2002) 629–635.
[7] T. Bermudez, S. Sammani, J.H. Song, V.R. Hernon, C.L. Kempf, A.N. Garcia, J. Burt, M. Hufford, S.M. Camp, A.E. Cress, A.A. Desai, V. Natarajan, J.R. Jacobson, S. M. Dudek, L.C. Cancio, J. Alvarez, R. Rafikov, Y. Li, D.D. Zhang, N.G. Casanova, C. Bime, J.G.N. Garcia, eNAMPT neutralization reduces preclinical ARDS severity via rectified NFkB and Akt/mTORC2 signaling, Sci. Rep. 12 (2022) 696.
[8] S. Sammani, T. Bermudez, C.L. Kempf, J.H. Song, J.C. Fleming, V. Reyes Hernon, M. Hufford, L. Tang, H. Cai, S.M. Camp, V. Natarajan, J.R. Jacobson, S.M. Dudek, D.R. Martin, C. Karmonik, X. Sun, B. Sun, N.G. Casanova, C. Bime, J.G.N. Garcia, eNAMPT neutralization preserves lung fluid balance and reduces acute renal injury in porcine Sepsis/VILI-induced inflammatory lung injury, Front. Physiol. 13 (2022), 916159.
[9] C. Bime, N.G. Casanova, J. Nikolich-Zugich, K.S. Knox, S.M. Camp, J.G.N. Garcia, Strategies to DAMPen COVID-19-mediated lung and systemic inflammation and vascular injury, Transl. Res. 232 (2021) 37–48.
[10] V.R. Elangovan, S.M. Camp, G.T. Kelly, A.A. Desai, D. Adyshev, X. Sun, S.M. Black, T. Wang, J.G. Garcia, Endotoxin- and mechanical stress-induced epigenetic changes in the regulation of the nicotinamide phosphoribosyltransferase promoter, Pulm. Circ. 6 (2016) 539–544.
[11] H. Quijada, T. Bermudez, C.L. Kempf, D.G. Valera, A.N. Garcia, S.M. Camp, J. H. Song, E. Franco, J.K. Burt, B. Sun, J.B. Mascarenhas, K. Burns, A. Gaber, R. C. Oita, V. Reyes Hernon, C. Barber, L. Moreno-Vinasco, X. Sun, A.E. Cress, D. Martin, Z. Liu, A.A. Desai, V. Natarajan, J.R. Jacobson, S.M. Dudek, C. Bime, S. Sammani, J.G.N. Garcia, Endothelial eNAMPT amplifies pre-clinical acute lung injury: efficacy of an eNAMPT-neutralising monoclonal antibody, Eur. Respir. J. 57 (2021).
[12] J. Geng, Y. Shi, J. Zhang, B. Yang, P. Wang, W. Yuan, H. Zhao, J. Li, F. Qin, L. Hong, C. Xie, X. Deng, Y. Sun, C. Wu, L. Chen, D. Zhou, TLR4 signalling via Piezo1 engages and enhances the macrophage mediated host response during bacterial infection, Nat. Commun. 12 (2021) 3519.
[13] B.M. Babior, The NADPH oxidase of endothelial cells, IUBMB Life 50 (2000) 267–269.
[14] G.M. Bokoch, Regulation of the human neutrophil NADPH oxidase by the rac GTP-binding proteins, Curr. Opin. Cell Biol. 6 (1994) 212–218.
[15] P.L. Hordijk, Regulation of NADPH oxidases: the role of rac proteins, Circ. Res. 98 (2006) 453–462.
[16] E. Monaghan-Benson, K. Burridge, The regulation of vascular endothelial growth factor-induced microvascular permeability requires rac and reactive oxygen species, J. Biol. Chem. 284 (2009) 25602–25611.
[17] J. Jiang, K. Huang, S. Xu, J.G.N. Garcia, C. Wang, H. Cai, Targeting NOX4 alleviates sepsis-induced acute lung injury via attenuation of redox-sensitive activation of CaMKII/ERK1/2/MLCK and endothelial cell barrier dysfunction, Redox Biol. 36 (2020), 101638.
[18] S. Palumbo, Y.J. Shin, K. Ahmad, A.A. Desai, H. Quijada, M. Mohamed, A. Knox, S. Sammani, B.A. Colson, T. Wang, J.G. Garcia, L. Hecker, Dysregulated Nox4 ubiquitination contributes to redox imbalance and age-related severity of acute lung injury, Am. J. Phys. Lung Cell. Mol. Phys. 312 (2017) L297–L308.
[19] M. Rojo de la Vega, M. Dodson, C. Gross, H.M. Mansour, R.C. Lantz, E. Chapman, T. Wang, S.M. Black, J.G. Garcia, D.D. Zhang, Role of Nrf2 and autophagy in acute lung injury, Curr. Pharmacol. Rep. 2 (2016) 91–101.
[20] P.A. Singleton, S.M. Dudek, E.T. Chiang, J.G. Garcia, Regulation of sphingosine 1-phosphate-induced endothelial cytoskeletal rearrangement and barrier enhancement by S1P1 receptor, PI3 kinase, Tiam1/Rac1, and alpha-actinin, FASEB J. 19 (2005) 1646–1656.
[21] P.A. Singleton, R. Salgia, L. Moreno-Vinasco, J. Moitra, S. Sammani, T. Mirzapoiazova, J.G. Garcia, CD44 regulates hepatocyte growth factor-mediated vascular integrity. Role of c-met, Tiam1/Rac1, dynamin 2, and cortactin, J. Biol. Chem. 282 (2007) 30643–30657.
[22] A.A. Birukova, S. Chatchavalvanich, A. Rios, K. Kawkitinarong, J.G. Garcia, K. G. Birukov, Differential regulation of pulmonary endothelial monolayer integrity by varying degrees of cyclic stretch, Am. J. Pathol. 168 (2006) 1749–1761.
[23] B. Wojciak-Stothard, A.J. Ridley, Rho GTPases and the regulation of endothelial permeability, Vasc. Pharmacol. 39 (2002) 187–199.
[24] S.M. Dudek, E.T. Chiang, S.M. Camp, Y. Guo, J. Zhao, M.E. Brown, P.A. Singleton, L. Wang, A. Desai, F.T. Arce, R. Lal, J.E. Van Eyk, S.Z. Imam, J.G. Garcia, Abl tyrosine kinase phosphorylates nonmuscle myosin light chain kinase to regulate endothelial barrier function, Mol. Biol. Cell 21 (2010) 4042–4056.
[25] T. Wang, M.E. Brown, G.T. Kelly, S.M. Camp, J.B. Mascarenhas, X. Sun, S. M. Dudek, J.G.N. Garcia, Myosin light chain kinase (MYLK) coding polymorphisms modulate human lung endothelial cell barrier responses via altered tyrosine phosphorylation, spatial localization, and lamellipodial protrusions, Pulm. Circ. 8 (2018), 2045894018764171.
[26] A.J. Ridley, H.F. Paterson, C.L. Johnston, D. Diekmann, A. Hall, The small GTP-binding protein rac regulates growth factor-induced membrane ruffling, Cell 70 (1992) 401–410.
[27] V. Spindler, N. Schlegel, J. Waschke, Role of GTPases in control of microvascular permeability, Cardiovasc. Res. 87 (2010) 243–253.
[28] A. Eriksson, R. Cao, J. Roy, K. Tritsaris, C. Wahlestedt, S. Dissing, J. Thyberg, Y. Cao, Small GTP-binding protein rac is an essential mediator of vascular endothelial growth factor-induced endothelial fenestrations and vascular permeability, Circulation 107 (2003) 1532–1538.
[29] Y. Wang, F. Yan, Q. Ye, X. Wu, F. Jiang, PTP1B inhibitor promotes endothelial cell motility by activating the DOCK180/Rac1 pathway, Sci. Rep. 6 (2016) 24111.
[30] E. Kiyokawa, Y. Hashimoto, S. Kobayashi, H. Sugimura, T. Kurata, M. Matsuda, Activation of Rac1 by a crk SH3-binding protein, DOCK180, Genes Dev. 12 (1998) 3331–3336.
[31] E. Brugnera, L. Haney, C. Grimsley, M. Lu, S.F. Walk, A.C. Tosello-Trampont, I. G. Macara, H. Madhani, G.R. Fink, K.S. Ravichandran, Unconventional rac-GEF activity is mediated through the Dock180-ELMO complex, Nat. Cell Biol. 4 (2002) 574–582.
[32] D. Komander, M. Patel, M. Laurin, N. Fradet, A. Pelletier, D. Barford, J.F. Cote, An alpha-helical extension of the ELMO1 pleckstrin homology domain mediates direct interaction to DOCK180 and is critical in rac signaling, Mol. Biol. Cell 19 (2008) 4837–4851.
[33] F. Sanematsu, M. Hirashima, M. Laurin, R. Takii, A. Nishikimi, K. Kitajima, G. Ding, M. Noda, Y. Murata, Y. Tanaka, S. Masuko, T. Suda, C. Meno, J.F. Cote, T. Nagasawa, Y. Fukui, DOCK180 is a rac activator that regulates cardiovascular development by acting downstream of CXCR4, Circ. Res. 107 (2010) 1102–1105.
[34] C.L. Kempf, S. Sammani, T. Bermudez, J.H. Song, V.R. Hernon, M.K. Hufford, J. Burt, S.M. Camp, S.M. Dudek, J.G.N. Garcia, Critical role for the lung endothelial nonmuscle myosin light-chain kinase isoform in the severity of inflammatory murine lung injury, Pulm. Circ. 12 (2022), e12061.
[35] J.H. Song, K. Kandasamy, M. Zemskova, Y.W. Lin, A.S. Kraft, The BH3 mimetic ABT-737 induces cancer cell senescence, Cancer Res. 71 (2011) 506–515.
[36] A. Garcia Ponce, A.F. Citalan Madrid, H. Vargas Robles, S. Chanez Paredes, P. Nava, A. Betanzos, A. Zarbock, K. Rottner, D. Vestweber, M. Schnoor, Loss of

cortactin causes endothelial barrier dysfunction via disturbed adrenomedullin secretion and actomyosin contractility, Sci. Rep. 6 (2016) 29003.
[37] J.R. Jacobson, S.M. Dudek, P.A. Singleton, I.A. Kolosova, A.D. Verin, J.G. Garcia, Endothelial cell barrier enhancement by ATP is mediated by the small GTPase rac and cortactin, Am. J. Phys. Lung Cell. Mol. Phys. 291 (2006) L289–L295.
[38] S.Q. Ye, B.A. Simon, J.P. Maloney, A. Zambelli-Weiner, L. Gao, A. Grant, R. B. Easley, B.J. McVerry, R.M. Tuder, T. Standiford, R.G. Brower, K.C. Barnes, J. G. Garcia, Pre-B-cell colony-enhancing factor as a potential novel biomarker in acute lung injury, Am. J. Respir. Crit. Care Med. 171 (2005) 361–370.
[39] S. Mandala, R. Hajdu, J. Bergstrom, E. Quackenbush, J. Xie, J. Milligan, R. Thornton, G.J. Shei, D. Card, C. Keohane, M. Rosenbach, J. Hale, C.L. Lynch, K. Rupprecht, W. Parsons, H. Rosen, Alteration of lymphocyte trafficking by sphingosine-1-phosphate receptor agonists, Science 296 (2002) 346–349.
[40] S.M. Dudek, S.M. Camp, E.T. Chiang, P.A. Singleton, P.V. Usatyuk, Y. Zhao, V. Natarajan, J.G. Garcia, Pulmonary endothelial cell barrier enhancement by FTY720 does not require the S1P1 receptor, Cell. Signal. 19 (2007) 1754–1764.
[41] L. Wang, E.T. Chiang, J.T. Simmons, J.G. Garcia, S.M. Dudek, FTY720-induced human pulmonary endothelial barrier enhancement is mediated by c-abl, Eur. Respir. J. 38 (2011) 78–88.
[42] H. Esterbauer, R.J. Schaur, H. Zollner, Chemistry and biochemistry of 4-hydroxy-nonenal, malonaldehyde and related aldehydes, Free Radic. Biol. Med. 11 (1991) 81–128.
[43] I. Rahman, A.A. van Schadewijk, A.J. Crowther, P.S. Hiemstra, J. Stolk, W. MacNee, W.I. De Boer, 4-Hydroxy-2-nonenal, a specific lipid peroxidation product, is elevated in lungs of patients with chronic obstructive pulmonary disease, Am. J. Respir. Crit. Care Med. 166 (2002) 490–495.
[44] P. Belvitch, Y.M. Htwe, M.E. Brown, S. Dudek, Cortical actin dynamics in endothelial permeability, Curr. Top. Membr. 82 (2018) 141–195.
[45] J.G. Garcia, F. Liu, A.D. Verin, A. Birukova, M.A. Dechert, W.T. Gerthoffer, J. R. Bamberg, D. English, Sphingosine 1-phosphate promotes endothelial cell barrier integrity by edg-dependent cytoskeletal rearrangement, J. Clin. Invest. 108 (2001) 689–701.
[46] B.J. McVerry, X. Peng, P.M. Hassoun, S. Sammani, B.A. Simon, J.G. Garcia, Sphingosine 1-phosphate reduces vascular leak in murine and canine models of acute lung injury, Am. J. Respir. Crit. Care Med. 170 (2004) 987–993.
[47] J.G. Garcia, H.W. Davis, C.E. Patterson, Regulation of endothelial cell gap formation and barrier dysfunction: role of myosin light chain phosphorylation, J. Cell. Physiol. 163 (1995) 510–522.
[48] M. Ikebe, D.J. Hartshorne, Phosphorylation of smooth muscle myosin at two distinct sites by myosin light chain kinase, J. Biol. Chem. 260 (1985) 10027–10031.
[49] K. Kimura, M. Ito, M. Amano, K. Chihara, Y. Fukata, M. Nakafuku, B. Yamamori, J. Feng, T. Nakano, K. Okawa, A. Iwamatsu, K. Kaibuchi, Regulation of myosin phosphatase by Rho and Rho-associated kinase (Rho-kinase), Science 273 (1996) 245–248.
[50] S.M. Camp, E. Ceco, C.L. Evenoski, S.M. Danilov, T. Zhou, E.T. Chiang, L. Moreno-Vinasco, B. Mapes, J. Zhao, G. Gursoy, M.E. Brown, D.M. Adyshev, S.S. Siddiqui, H. Quijada, S. Sammani, E. Letsiou, L. Saadat, M. Yousef, T. Wang, J. Liang, J. G. Garcia, Unique toll-like receptor 4 activation by NAMPT/PBEF induces NFkappaB signaling and inflammatory lung injury, Sci. Rep. 5 (2015) 13135.
[51] T.L. Gumienny, E. Brugnera, A.C. Tosello-Trampont, J.M. Kinchen, L.B. Haney, K. Nishiwaki, S.F. Walk, M.E. Nemergut, I.G. Macara, R. Francis, T. Schedl, Y. Qin, L. Van Aelst, M.O. Hengartner, K.S. Ravichandran, CED-12/ELMO, a novel member of the CrkII/Dock180/Rac pathway, is required for phagocytosis and cell migration, Cell 107 (2001) 27–41.
[52] H. Tajiri, T. Uruno, T. Shirai, D. Takaya, S. Matsunaga, D. Setoyama, M. Watanabe, M. Kukimoto-Niino, K. Oisaki, M. Ushijima, F. Sanematsu, T. Honma, T. Terada, E. Oki, S. Shirasawa, Y. Maehara, D. Kang, J.F. Cote, S. Yokoyama, M. Kanai, Y. Fukui, Targeting ras-driven cancer cell survival and invasion through selective inhibition of DOCK1, Cell Rep. 19 (2017) 969–980.
[53] C. Bime, T. Zhou, T. Wang, M.J. Slepian, J.G. Garcia, L. Hecker, Reactive oxygen species-associated molecular signature predicts survival in patients with sepsis, Pulm. Circ. 6 (2016) 196–201.
[54] S. Aggarwal, C. Dimitropoulou, Q. Lu, S.M. Black, S. Sharma, Glutathione supplementation attenuates lipopolysaccharide-induced mitochondrial dysfunction and apoptosis in a mouse model of acute lung injury, Front. Physiol. 3 (2012) 161.
[55] M.D. Howard, C.F. Greineder, E.D. Hood, V.R. Muzykantov, Endothelial targeting of liposomes encapsulating SOD/catalase mimetic EUK-134 alleviates acute pulmonary inflammation, J. Control. Release 177 (2014) 34–41.
[56] P.G. Metnitz, C. Bartens, M. Fischer, P. Fridrich, H. Steltzer, W. Druml, Antioxidant status in patients with acute respiratory distress syndrome, Intensive Care Med. 25 (1999) 180–185.
[57] Z. Sun, Z. Niu, S. Wu, S. Shan, Protective mechanism of sulforaphane in Nrf2 and anti-lung injury in ARDS rabbits, Exp. Ther. Med. 15 (2018) 4911–4915.
[58] P.M. Suter, G. Domenighetti, M.D. Schaller, M.C. Laverriere, R. Ritz, C. Perret, N-acetylcysteine enhances recovery from acute lung injury in man. A randomized, double-blind, placebo-controlled clinical study, Chest 105 (1994) 190–194.
[59] S. Tao, M. Rojo de la Vega, H. Quijada, G.T. Wondrak, T. Wang, J.G. Garcia, D. D. Zhang, Bixin protects mice against ventilation-induced lung injury in an NRF2-dependent manner, Sci. Rep. 6 (2016) 18760.
[60] N.M. Reddy, S.R. Kleeberger, T.W. Kensler, M. Yamamoto, P.M. Hassoun, S. P. Reddy, Disruption of Nrf2 impairs the resolution of hyperoxia-induced acute lung injury and inflammation in mice, J. Immunol. 182 (2009) 7264–7271.
[61] H.Y. Cho, A.E. Jedlicka, S.P. Reddy, T.W. Kensler, M. Yamamoto, L.Y. Zhang, S. R. Kleeberger, Role of NRF2 in protection against hyperoxic lung injury in mice, Am. J. Respir. Cell Mol. Biol. 26 (2002) 175–182.
[62] S. Papaiahgari, A. Yerrapureddy, S.R. Reddy, N.M. Reddy, O.J. Dodd, M.T. Crow, D.N. Grigoryev, K. Barnes, R.M. Tuder, M. Yamamoto, T.W. Kensler, S. Biswal, W. Mitzner, P.M. Hassoun, S.P. Reddy, Genetic and pharmacologic evidence links oxidative stress to ventilator-induced lung injury in mice, Am. J. Respir. Crit. Care Med. 176 (2007) 1222–1235.
[63] P. Fu, Y. Epshtein, R. Ramchandran, J.B. Mascarenhas, A.E. Cress, J. Jacobson, J.G. N. Garcia, V. Natarajan, Essential role for paxillin tyrosine phosphorylation in LPS-induced mitochondrial fission, ROS generation and lung endothelial barrier loss, Sci. Rep. 11 (2021) 17546.
[64] E. Kratzer, Y. Tian, N. Sarich, T. Wu, A. Meliton, A. Leff, A.A. Birukova, Oxidative stress contributes to lung injury and barrier dysfunction via microtubule destabilization, Am. J. Respir. Cell Mol. Biol. 47 (2012) 688–697.
[65] H.S. Park, H.Y. Jung, E.Y. Park, J. Kim, W.J. Lee, Y.S. Bae, Cutting edge: direct interaction of TLR4 with NAD(P)H oxidase 4 isozyme is essential for lipopolysaccharide-induced production of reactive oxygen species and activation of NF-kappa B, J. Immunol. 173 (2004) 3589–3593.
[66] Y. Shikata, K.G. Birukov, J.G. Garcia, S1P induces FA remodeling in human pulmonary endothelial cells: role of Rac, GIT1, FAK, and paxillin, J. Appl. Physiol. (1985) 94 (2003) 1193–1203.